

Article

Microscopic Processes in Global Relativistic Jets Containing Helical Magnetic Fields: Dependence on Jet Radius

Ken-Ichi Nishikawa ^{1,*}, Yosuke Mizuno ², Jose L. Gómez ³, Ioana Duțan ⁴, Athina Meli ^{5,6}, Charley White ⁷, Jacek Niemiec ⁸, Oleh Kobzar ⁸, Martin Pohl ^{9,10}, Asaf Pe'er ¹¹, Jacob Trier Frederiksen ¹², Åke Nordlund ¹³, Helene Sol ¹⁴, Philip E. Hardee ¹⁵ and Dieter H. Hartmann ¹⁶

- ¹ Department of Physics, University of Alabama in Huntsville, ZP12, Huntsville, AL 35899, USA
- ² Institute for Theoretical Physics, Goethe University, Frankfurt am Main D-60438, Germany; mizuno@th.physik.uni-frankfurt.de
- ³ Instituto de Astrofísica de Andalucía, CSIC, Apartado 3004, Granada 18080, Spain; jlgomez@iaa.csic.es
- ⁴ Institute of Space Science, Atomistilor 409, Bucharest-Magurele RO-077125, Romania; ioana.dutan@gmail.com
- ⁵ Department of Physics and Astronomy, University of Gent, Proeftuinstraat 86, Gent B-9000, Belgium
- ⁶ Department of Physics and Astronomy, University of Liege, Place du 20-Août, 7 4000 Liège, Belgium; ameli@ulg.ac.be
- ⁷ Department of Physics, University of Alabama in Huntsville, Huntsville, AL 35899, USA; cmw0037@uah.edu
- ⁸ Institute of Nuclear Physics PAN, ul. Radzikowskiego 152, Kraków 31-342, Poland; Jacek.Niemiec@ifj.edu.pl (J.N.); oleh.kobzar@ifj.edu.pl(O.K.)
- ⁹ Institut für Physik und Astronomie, Universität Potsdam, Potsdam-Golm 14476, Germany; pohlmadq@gmail.com
- ¹⁰ DESY, Platanenallee 6, Zeuthen 15738, Germany; pohlmadq@gmail.com
- ¹¹ Physics Department, University College Cork, Cork T12 YN60, Ireland; a.peer@ucc.ie
- ¹² Innofactor Denmark A/S, Telia Parken, Øster Allé 48, 2100 København Ø, Denmark; jacob.trier@innofactor.com
- ¹³ Niels Bohr Institute, University of Copenhagen, Blegdamsvej 17, København DK-2100, Denmark; aake@nbi.dk
- ¹⁴ LUTH, Observatoire de Paris-Meudon, 5 place Jules Jansen, Meudon Cedex 92195, France; helene.sol@obspm.fr
- ¹⁵ Department of Physics and Astronomy, The University of Alabama, Tuscaloosa, AL 35487, USA; pehardee@gmail.com
- ¹⁶ Department of Physics and Astronomy, Clemson University, Clemson, SC 29634, USA; hdieter@g.clemson.edu
- * Correspondence: ken-ichi.nishikawa@nasa.gov; Tel.: +1-256-824-2593
- † Current address: Affiliation 7: Department of Physics Florida State University 600 W. College Avenue Tallahassee, FL 32306, USA
- ‡ These authors contributed equally to this work.

Academic Editor: Emmanouil Angelakis, Markus Boettcher Jose L. Gómez

Received: date; Accepted: date; Published: date

Abstract: In this study we investigate jet interaction at a microscopic level in a cosmological environment, which responds to a key open question in the study of relativistic jets. Using small simulation systems during prior research, we initially studied the evolution of both electron-proton and electron-positron relativistic jets containing helical magnetic fields, by focusing on their interactions with an ambient plasma. Here, using larger jet radii, we have performed simulations of global jets containing helical magnetic fields in order to examine how helical magnetic fields affect kinetic instabilities such as the Weibel instability, the kinetic Kelvin-Helmholtz instability (kKHI) and the Mushroom instability (MI). We found that the evolution of global jets strongly depends on the size of the jet radius. For example, phase bunching of jet electrons, in particular

in the electron-proton jet, is mixed with larger jet radius due to the more complicated structures of magnetic fields with excited kinetic instabilities. In our simulation study these kinetic instabilities lead to new types of instabilities in global jets. In the electron-proton jet simulation a modified recollimation occurs and jet electrons are strongly perturbed. In the electron-positron jet simulation mixed kinetic instabilities occur at early times followed by a turbulence-like structure. Simulations using much larger (and longer) systems are further required in order to thoroughly investigate the evolution of global jets containing helical magnetic fields.

Keywords: relativistic jets; particle-in-cell simulations; global jets; helical magnetic fields; kinetic instabilities; kink-like instability; recollimation shocks; polarized radiation

1. Introduction

Relativistic jets are collimated plasma outflows associated with active galactic nuclei (AGN), gamma-ray bursts (GRBs), and pulsars (e.g., [1]). Among these astrophysical systems, blazars and GRB jets produce the most luminous phenomena in the universe (e.g., [2]). Despite extensive observational and theoretical investigations, including simulation studies, our understanding of their formation, their interaction and evolution in the ambient plasma, and consequently their observable properties such as time-dependent flux and polarity (e.g., [3]), remains quite limited.

Astrophysical jets are ubiquitous in the universe and provide many essential plasma phenomena such as interaction with interstellar medium, generation of magnetic fields, turbulence, reconnection and particle acceleration. Many of the processes that determine the behavior of global relativistic jets are very complex, involving plasma physics and often coupling global, large-scale dynamics to microscopic processes that occur on short spatial and temporal scales associated with plasma kinetic effects. We have carried out kinetic plasma simulations using our relativistic particle-in-cell (RPIC) code, with the intent to advance our knowledge of global relativistic jets with helical magnetic fields and associated phenomena such as particle acceleration, kinetic reconnection and turbulence, which cannot be investigated with fluid models (i.e., relativistic magnetohydrodynamic (RMHD) simulations).

Recently, we performed “global” jet simulations involving the injection of a cylindrical unmagnetized jet into an ambient plasma in order to investigate shock (Weibel instability) and velocity shear instabilities (kKHI and Mushroom instability (MI)) simultaneously [4]. In this paper we will describe the preliminary results of this new study of global relativistic jets containing helical magnetic fields.

2. Simulation Setups of Global Jet Simulations

Jets generated from black holes, which are then injected into the ambient interstellar medium contain magnetic fields that are thought to be helically twisted. Based on this understanding, we performed global simulations of jets containing helical magnetic fields injected into an ambient medium (e.g., [5,6]). The key issue we investigated is how the helical magnetic fields affect the growth of the kKHI, the MI, and the Weibel instability. RMHD simulations demonstrated that jets containing helical magnetic fields develop kink instability (e.g., [7–9]). Since our RPIC simulations are large enough to include a kink instability, we found a kink-like instability in our electron-proton jet case.

2.1. Helical Magnetic Field Structure

In our simulations [5], cylindrical jets are injected with a helical magnetic field implemented like that in RMHD simulations performed by Mizuno et al. [10]. Our simulations use Cartesian

coordinates. Since $\alpha = 1$, Equations (9)–(11) from [10] are reduced to Equation (1), and the magnetic field takes the form:

$$B_x = \frac{B_0}{[1 + (r/a)^2]}, \quad B_\phi = \frac{(r/a)B_0}{[1 + (r/a)^2]} \quad (1)$$

The toroidal magnetic field is created by a current $+J_x(y, z)$ in the positive x -direction, so that defined in Cartesian coordinates:

$$B_y(y, z) = \frac{((z - z_{jc})/a)B_0}{[1 + (r/a)^2]}, \quad B_z(y, z) = -\frac{((y - y_{jc})/a)B_0}{[1 + (r/a)^2]}. \quad (2)$$

Here a is the characteristic length-scale of the helical magnetic field, (y_{jc}, z_{jc}) is the center of the jet, and $r = \sqrt{(y - y_{jc})^2 + (z - z_{jc})^2}$. The chosen helicity is defined through Equation (2), which has a left-handed polarity with positive B_0 . At the jet orifice, we implement the helical magnetic field without the motional electric fields. This corresponds to a toroidal magnetic field generated self-consistently by jet particles moving along the $+x$ -direction.

2.2. Magnetic Fields in Helically Magnetized RPIC Jets with Larger Jet Radius

As an initial step, we examined how the helical magnetic field modifies jet evolution using a small system before performing larger-scale simulations. A schematic of the simulation injection setup is used in our previous work [5]. In these small system simulations, we utilized a numerical grid with $(L_x, L_y, L_z) = (645\Delta, 131\Delta, 131\Delta)$ (simulation cell size: $\Delta = 1$) and periodic boundary conditions in transverse directions with jet radius $r_{jt} = 20\Delta$. The jet and ambient (electron) plasma number density measured in the simulation frame is $n_{jt} = 8$ and $n_{am} = 12$, respectively. This set of densities of jet and ambient plasmas is used in our previous simulations [4–6]

In the simulations, the electron skin depth $\lambda_s = c/\omega_{pe} = 10.0\Delta$, where c is the speed of light, $\omega_{pe} = (e^2 n_{am} / \epsilon_0 m_e)^{1/2}$ is the electron plasma frequency, and the electron Debye length for the ambient electrons is $\lambda_D = 0.5\Delta$. The jet–electron thermal velocity is $v_{jt,th,e} = 0.014c$ in the jet reference frame. The electron thermal velocity in the ambient plasma is $v_{am,th,e} = 0.03c$, and ion thermal velocities are smaller by $(m_i/m_e)^{1/2}$. Simulations were performed using an electron–positron (e^\pm) plasma or an electron–proton ($e^- - p^+$ with $m_p/m_e = 1836$) plasma for the jet Lorentz factor of 15 and with the ambient plasma at rest ($v_{am} = 0$).

In the simulations we use the initial magnetic field amplitude parameter $B_0 = 0.1c$, ($c = 1$), ($\sigma = B^2/n_e m_e \gamma_{jet} c^2 = 2.8 \times 10^{-3}$), and $a = 0.25 * r_{jt}$. The helical field structure inside the jet is defined by Equations (1) and (2). For the external magnetic fields, we use a damping function $\exp[-(r - r_{jt})^2/b]$ ($r \geq r_{jt}$) that multiplies Equations (1) and (2) with the tapering parameter $b = 200$. The final profiles of the helical magnetic field components are similar to that in the case where jet radius $r_{jt} = 20\Delta$, the only difference is $a = 0.25 * r_{jt}$.

In this report we maintain all simulation parameters as described above except jet radius and simulation size (adjusted based on the jet radius). We have performed simulations with larger jet radii $r_{jt} = 40\Delta, 80\Delta, \text{ and } 120\Delta$. In these small system simulations, we utilize a numerical grid with $(L_x, L_y, L_z) = (645\Delta, 257\Delta, 257\Delta), (645\Delta, 509\Delta, 509\Delta), (645\Delta, 761\Delta, 761\Delta)$ (simulation cell size: $\Delta = 1$). The cylindrical jet with jet radius $r_{jt} = 40\Delta, 80\Delta, \text{ and } 120\Delta$ is injected in the middle of the $y - z$ plane ($(y_{jc}, z_{jc}) = (129\Delta, 129\Delta), (252\Delta, 252\Delta), (381\Delta, 381\Delta)$) at $x = 100\Delta$, respectively. The largest jet radius ($r_{jt} = 120\Delta$) is larger than that ($r_{jt} = 100\Delta$) in [4], but the simulation length is much shorter ($x = 2005\Delta$).

Figure 1 shows the y component of the magnetic field (B_y) in the jet radius with $r_{jet} = 20\Delta$ and 80Δ . The initial helical magnetic field (left-handed; clockwise viewed from the jet front) is enhanced and disrupted due to the instabilities for both cases.

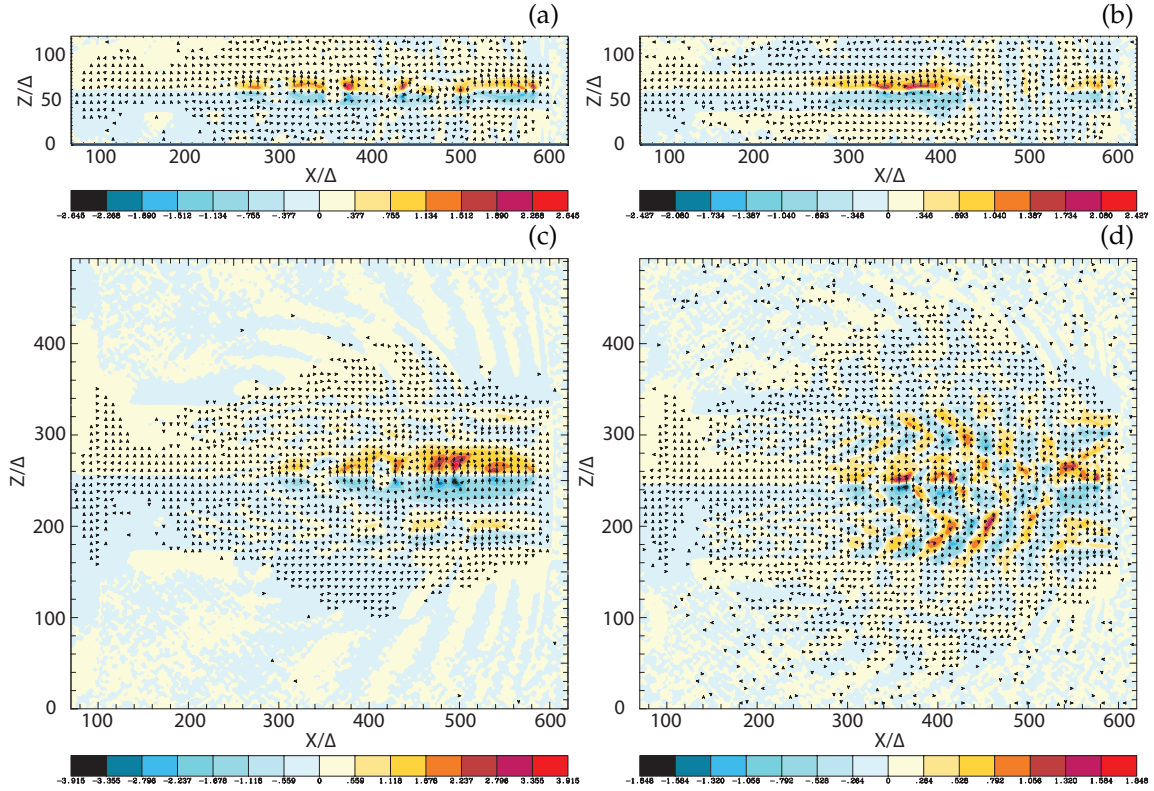


Figure 1. Isocontour plots of the azimuthal component of magnetic field B_y intensity at the center of the jets for $e^- - p^+$ ((a) and (c)) and e^\pm ((b) and (d)) jets; with $r_{\text{jet}} = 20\Delta$ ((a) and (b)) $r_{\text{jet}} = 80\Delta$ ((c) and (d)) at time $t = 500\omega_{\text{pe}}^{-1}$. The disruption of helical magnetic fields are caused by instabilities and/or reconnection. The max/min numbers of panels are (a) ± 2.645 , (b) ± 2.427 , (c) ± 3.915 , (d) ± 1.848 .

Even as a result of shorter simulation systems, the growing instabilities are affected by the helical magnetic fields. These complicated patterns of B_y are generated by the currents generated by instabilities in jets. The larger jet radius contributes more modes of instabilities to grow in the jets, which make the jet structures more complicated. The simple recollimation shock generated in the small jet radius is shown in Figs. 1(a) and 1(b) [5]. We need to perform longer simulations in order to investigate full development of instabilities and jets with helical magnetic fields.

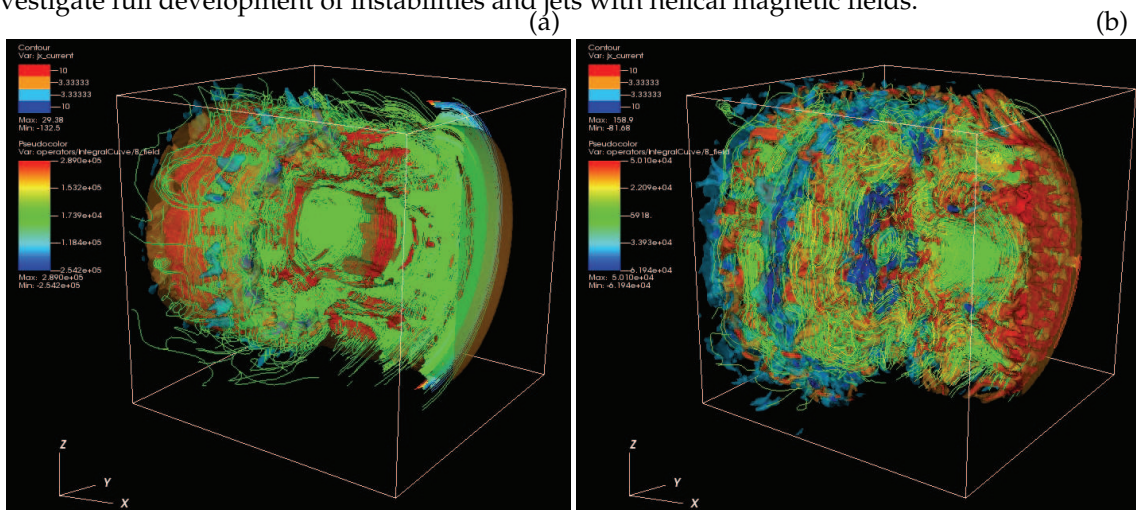


Figure 2. Panels show 3D iso-surface plots of the current (J_x) of jet electrons for $e^- - p^+$ (a) and e^\pm (b) jet with $r_{\text{jet}} = 80\Delta$ at time $t = 500\omega_{\text{pe}}^{-1}$. The lines show the magnetic field stream lines in the quadrant of the front part of jets. The color scales for contour (upper left) for (a) and (b): red 10; orange 3.33; right blue -3.33 . blue -10 . The color scales of streaming lines (a) $(2.89, 1.53, 0.174, -1.2, -2.54) \times 10^5$; (b) $(5.01, 2.21, -0.592, -3.39, -6.19) \times 10^4$.

In order to investigate 3D structures of averaged jet electron current (J_x) we plot it in the 3D ($420 \leq x/\Delta \leq 620, 152 \leq y, z/\Delta \leq 352$) region of the jet front.

Figure 2 shows the current (J_x) of jet electrons for $e^- - p^+$ (a) and e^\pm (b) jets. The cross sections at $x/\Delta = 520, y/\Delta = 252$ and surfaces of jets show complicated patterns, which are generated by instabilities with the magnetic field lines.

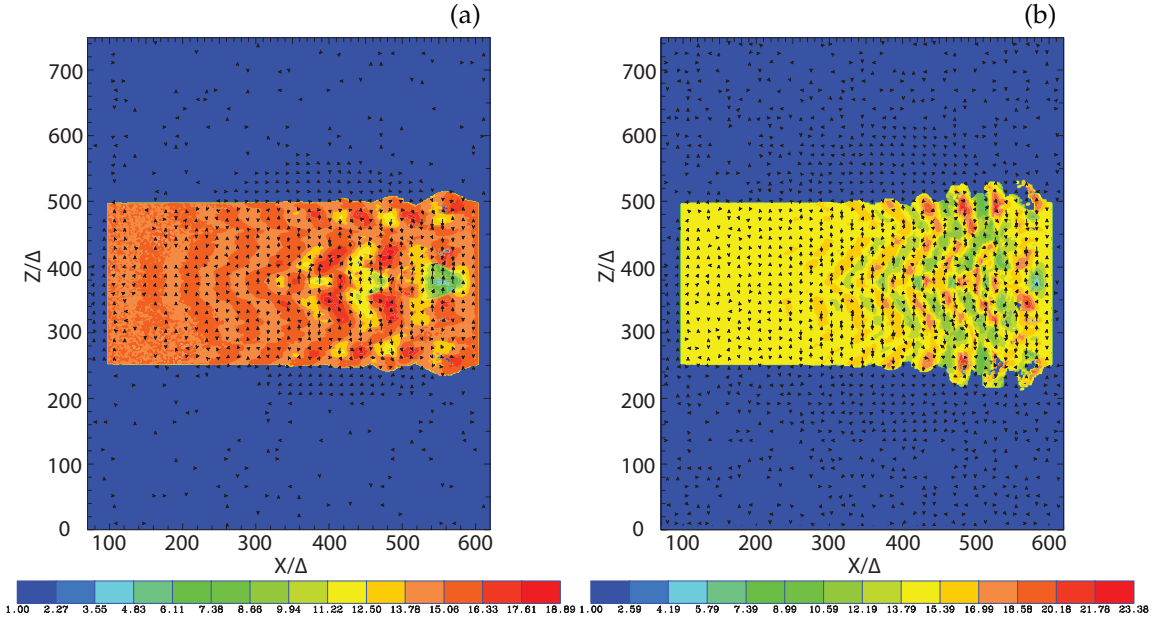


Figure 3. Panels (a) and (b) show 2D plot of the Lorentz factor of jet electrons for $e^- - p^+$ (a) and e^\pm (b) jet with $r_{\text{jet}} = 120\Delta$ at time $t = 500\omega_{\text{pe}}^{-1}$. The arrows (black spots) show the magnetic fields in the $x - z$ plane.

In order to determine particle acceleration we calculated the Lorentz factor of jet electrons in the cases with $r_{\text{jet}} = 120\Delta$ as shown in Fig. 3. These patterns of Lorentz factor coincide with the changing directions of local magnetic fields that are generated by instabilities. The directions of magnetic fields are indicated by the arrows (black spots), which can be seen with magnification. The directions of magnetic fields are determined by the generated instabilities. The structures at the edge of jets are generated by the kKHI. The plots of Lorentz factor in the $y - z$ plane show the MI in the circular edge of the jets (the x component of current J_x) as shown in Figure S1.

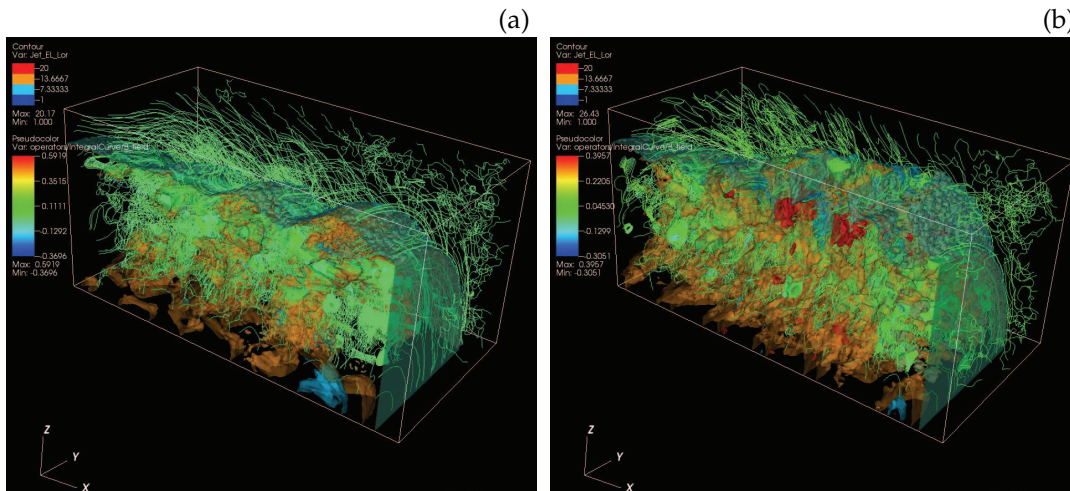


Figure 4. Panels show 3D iso-surface plots of the Lorentz factor of jet electrons for $e^- - p^+$ (a) and e^\pm (b) jet with $r_{\text{jet}} = 120\Delta$ at time $t = 500\omega_{\text{pe}}^{-1}$. The lines show the magnetic field stream lines in the quadrant of the front part of jets. The color scales for contour (upper left) for both (a) and (b): red 20.0; orange 13.67; right blue 7.33. blue 1. The color scales of streaming lines (a) $(5.92, 3.52, 0.174, -1.29, -3.70) \times 10^{-1}$; (b) $(3.96, 2.21, 0.453, -1.30, -3.05) \times 10^{-1}$.

In order to investigate 3D structures of the averaged jet electron Lorentz factor, we plot iso-surface of it in 3D ($320 \leq x/\Delta \leq 620$, $381 \leq y, z/\Delta \leq 531$) of a quadrant of the jet front.

Figure 4 shows the Lorentz factor of jet electrons for $e^- - p^+$ (a) and e^\pm (b) jet. The cross sections and surfaces of jets show complicated patterns that are generated by instabilities with the magnetic field lines.

In both cases with the jet radii larger than $r_{\text{jet}} = 80\Delta$, at the jet surfaces kKHI and MI are generated, and inside the jets the Weibel instability is generated with kink-like instability, in particular in the electron-proton jet. We aim to investigate further using different parameters including a , which determines the structure of helical magnetic fields in Equations (1) and (2).

3. Discussion

The global jet simulations with large jet radii show the importance of a larger jet radius in RPIC simulations for investigating in-tandem the macroscopic processes incorporated in RMHD simulations. Due to mixed modes of generated instabilities, jet electrons in phase space show little or no bunching in comparison to those with jet radius $r_{\text{jet}} = 20\Delta$ as shown in Figs. 5(a) and 5(b) in the previous report [5]. Consequently, recollimation shocks occur rather in the center of jets, which is dependent on the value of a in Eqs. (1) and (2). Further simulations with different values of a are required for investigating the evolution of kinetic instabilities in global jets.

These simulations show that the energy stored in helical magnetic fields is released due to the excitations of kinetic instabilities such as kKHI, MI and the Weibel instability with kink-like instability. Consequently, electrons are accelerated and turbulent magnetic fields are generated, which provide polarity.

MacDonald & Marscher [3] have developed a radiative transfer scheme that allows the Turbulent Extreme Multi-Zone (TEMZ) code to produce simulated images of the time-dependent linearly and circularly polarized intensity at different radio frequencies. Using this technique with our simulation results, we have produced synthetic polarized emission maps that highlight the linear and circular polarization expected within the model. We will discuss these findings in a separate paper.

We plan to perform additional simulations using a larger jet radius and longer systems in order to investigate the full dynamics of jet evolution and interaction with ambient mediums via developing instabilities.

Supplementary Materials: The following are available online at www.mdpi.com/link, Figure S1: title, Table S1: title, Video S1: title.

Acknowledgments: This work is supported by NSF AST-0908010, AST-0908040, NASA-NNX09AD16G, NNX12AH06G, NNX13AP-21G, and NNX13AP14G grants. The work of J.N. and O.K. has been supported by Narodowe Centrum Nauki through research project DEC-2013/10/E/ST9/00662. Y.M. is supported by the ERC Synergy Grant “BlackHoleCam - Imaging the Event Horizon of Black Holes” (Grant No. 610058). M.P. acknowledges support through grant PO 1508/1-2 of the Deutsche Forschungsgemeinschaft. Simulations were performed using Pleiades and Endeavor facilities at NASA Advanced Supercomputing (NAS), and using Gordon and Comet at The San Diego Supercomputer Center (SDSC), and Stampede at The Texas Advanced Computing Center, which are supported by the NSF. This research was started during the program “Chirps, Mergers and Explosions: The Final Moments of Coalescing Compact Binaries” at the Kavli Institute for Theoretical Physics, which is supported by the National Science Foundation under grant No. PHY05-51164. The first velocity shear results using an electron–positron plasma were obtained during the Summer Aspen workshop “Astrophysical Mechanisms of Particle Acceleration and Escape from the Accelerators” held at the Aspen Center for Physics (1–15 September 2013).

Author Contributions: K. -I. Nishikawa: Perform simulations, analyze the data and prepare a manuscript; Y. Mizuno: Compare with RMHD simulations; J. L. Gómez: Contribute for comparing simulation results to observations; J. Niemiec: Contribute modifying the code for this research; O. Kobzar: Modify the code for this simulation; M. Pohl: Overlook the simulation results; J. L. Gómez: Contribute on comparisons with observations; I. Duřan: Perform some of simulations for this research; A. Pe’er: Critical contributions for physical interpretation; J. T. Frederiksen: Contribution for critical discussions on this research; Å. Nordlund: Fruitful suggestions for this research; C. White: Contribute some simulations and discussions; A. Meli: Critical reading and discussion on this research; H. Sol: Essential suggestions for this research; P. E. Hardee: Theoretical contributions for this research; D. H. Hartmann: Useful discussions for this research

Conflicts of Interest: The authors declare no conflict of interest.

References

1. Hawley, J. F.; Fendt, C.; Hardcastle, M.; Nokhrina, E.; Tchekhovskoy, A.; Disks and Jets Gravity, Rotation and Magnetic Fields. *Space Sci. Rev.*, **2015**, *191*, 441–469.
2. Pe'er, A. Energetic and Broad Band Spectral Distribution of Emission from Astronomical Jets. *Space Sci. Rev.* **2014**, *183*, 371–403.
3. Nicholas R. MacDonald, M. R., & Marscher, A. P., Faraday Conversion in Turbulent Blazar Jets, *Astrophys. J.*, **2016**, submitted, (arXiv:1611.09954).
4. Nishikawa, K.-I.; Frederiksen, J.T.; Nordlund, Å.; Mizuno, Y.; Hardee, P.E.; Niemiec, J.; Gómez, J.L.; Pe'er, A.; Duğan, I.; Meli, A.; et al. Evolution of Global Relativistic Jets: Collimations and Expansion with kKHI and the Weibel Instability. *Astrophys. J.* **2016**, *820*, 94–107.
5. Nishikawa, K.-I.; Mizuno, Y.; Niemiec, J.; Kobzar, O.; Pohl, M.; Gómez, J. L.; Duğan, I.; Pe'er, A.; Frederiksen, J.T.; Nordlund, Å.; Meli, A.; Sol, H.; Hardee, P.E.; Hartmann, D.; Microscopic Processes in Global Relativistic Jets Containing Helical Magnetic Fields. *Galaxies* **2016**, *4*, 38–47.
6. Duğan, I., Nishikawa, K.-I., Mizuno, Y., Niemiec, J., Kobzar, O., Pohl, Pohl, M., Gómez, J. L., Pe'er, A., Frederiksen, J. T., Nordlund, A., Meli, A., Sol, H., Hardee, P. E., & Hartmann, D. H., Particle-in-cell Simulations of Global Relativistic Jets with Helical Magnetic Fields, *New Frontiers in Black Hole Astrophysics Proceedings IAU Symposium*, **2017**, *324*, 199–202.
7. Mizuno, Y.; Hardee, P. E.; Nishikawa, K.-I.; Spatial Growth of the Current-Driven Instability in Relativistic Jets, *ApJ*, **2014** *784* 167–182.
8. Singh, C. B.; Mizuno, Y.; de Gouveia Dal Pino, E. M.; Spatial Growth of Current-driven Instability in Relativistic Rotating Jets and the Search for Magnetic Reconnection. *ApJ*, **2016**, *824*, 48, 2016
9. Barniol Duran, R.; Tchekhovskoy, A.; Giannios, D.; Simulations of AGN jets: magnetic kink instability versus conical shocks. *Mon. Not. R. Astron. Soc.* **2017** *469*, 4957–4978.
10. Mizuno, Y.; Gómez, J.L.; Nishikawa, K.-I.; Meli, A.; Hardee, P.E.; Rezzolla, L. Recollimation Shocks in Magnetized Relativistic Jets. *Astrophys. J.* **2015**, *809*, 38.

Sample Availability: Data (vtk) for VisIt and ParaView are available upon the request.



© 2017 by the authors. Licensee MDPI, Basel, Switzerland. This article is an open access article distributed under the terms and conditions of the Creative Commons Attribution (CC BY) license (<http://creativecommons.org/licenses/by/4.0/>).